From Intracluster Planetary Nebulae to High-Redshift Lyα Emitters

R.P. KUDRITZKI and R.H. MÉNDEZ, Munich University Observatory
J.J. FELDMEIER and R. CIARDULLO, Dept. of Astron. and Astrophys., Penn State University
G.H. JACOBY, Kitt Peak National Observatory, Tucson
K.C. FREEMAN, Mt. Stromlo and Siding Spring Observatories
M. ARNABOLDI and M. CAPACCIOLI, Osservatorio Astronomico di Capodimonte, Napoli
O. GERHARD, Astronomisches Institut, Universität Basel
H.C. FORD, Physics and Astronomy Dept., Johns Hopkins University, Baltimore

1. Introduction

The fact that the spectra of planetary nebulae (PNs) are dominated by strong emission lines, with a very weak continuum, has two interesting consequences for extragalactic work. First, PNs in other galaxies are easily detectable: we need two images of a galaxy, one taken through a narrow-band filter transmitting a strong nebular emission (e.g. [O III] λ5007) and another taken through an off-band filter which does not transmit any strong nebular line. In the on-band image the PN appears as a point source. Since the nebular continuum is so weak, the point source should be invisible in the off-band image. By blinking the two images, and provided that the off-band image is deep enough, it is easy to identify the PNs. Second, for each detected PN we can measure an accurate radial velocity, because all the flux we have detected is concentrated at the redshifted wavelength of the emission line. Thus we can take a good spectrogram in an exposure time not much longer than what we need for the imaging. Since PNs are preferentially discovered in the outskirts of galaxies, where the surface brightness is lower, this means that PNs are ideal test particles for studies of rotation and mass distribution in the halos of the corresponding galaxies. Typical examples of such studies are Hui et al. (1995) on NGC 5128, and Arnaboldi et al. (1996) on the Virgo cluster galaxy NGC 4406. Here begins an unusual chain of unexpected results.

2. Intracluster PNs

The giant galaxy NGC 4406 is characterised by a negative redshift (–230 km s^{-1}), and indeed many of its PNs, discovered by Jacoby et al. (1990) and measured by Arnaboldi et al. (1996), have the expected redshifts. However, 3 of these PNs turn out to have redshifts typical of the Virgo cluster (around 1300 km s^{-1}). The conclusion was that these 3 PNs do not belong to NGC 4406; they must be members of an intergalactic or intracluster diffuse stellar population in the Virgo cluster, and only by chance they appear projected upon NGC 4406. Direct evidence of the existence of red giants belonging to this Virgo intracluster stellar population was subsequently reported by Ferguson et al. (1998), who worked with the Hubble Space Telescope. These red giants are too faint for spectroscopic studies. In contrast, the intracluster PNs offer an ideal opportunity to learn about the kinematic behaviour and perhaps even the abundances of the diffuse stellar population. A search for intracluster PNs in different positions across the Virgo cluster started immediately and produced dozens of PN candidates (Méndez et al. 1997, Feldmeier et al. 1998).

The “on-band/off-band” narrow-band filter technique used to discover the PN candidates allows the detection of a single emission line. This is not necessarily the desired [O III] λ5007; it might be another emission line at higher z, redshifted into the on-band filter, like [O II] λ3727 at z = 0.35, or Lyα at z = 3.14. In previous work (e.g. Méndez et al. 1997) we argued that most of our detections had to be real PNs because (a) the surface density of emission-line galaxies derived from previous studies (for example Thompson et al. 1995) was not high enough to explain all the detections; (b) the luminosity function of the detected sources, if we assume them to be at the distance of the Virgo cluster, is in good agreement with the PN luminosity functions derived in several Virgo galaxies (Jacoby et al. 1990).

Then we decided to take deep VLT+FORS spectrograms of several intracluster PN candidates, located in Field 1 of Feldmeier et al. (1998) and in the smaller field observed by Méndez et al. (1997; in what follows the “La Palma Field” or LPF, because the discovery images were taken with the 4.2-m William Herschel Telescope at La Palma). Our purpose was first of all to measure radial velocities and provide spectroscopic confirmation of the PN nature of the candidates, since a few of them could be high-redshift sources. Second, we were hoping to detect the very faint diagnostic emission lines necessary for reliable abundance determinations, at least for a few of the brightest intracluster PN candidates. This was not to be; in what follows we report the unexpected outcome of our first VLT run. Here we will restrict our description to the LPF, where the most interesting objects are located. A paper with a complete report has been submitted to *ApJ*.

3. Observations and First Results

In April 1999 we used the VLT UT1 with FORS in multi-object spectroscopic mode (MOS) with grism 300V. We defined 1 arcsec wide slitlets for several PN candidates in the LPF, and added slitlets for 2 objects suspected to be QSOs or starbursts because they were visible (although much weaker) in the off-band discovery image (Méndez et al. 1997). Some other slitlets were placed on stars or galaxies in the field, in order to check the slitlet positioning (done by taking a short exposure without grism through the slitlets) and to help locate the dispersion lines as a function of position across the field, which is important for the correct extraction of spectra consisting of isolated emission lines.

After completing 5 exposures of the initial MOS configuration, each 40 minutes long, the surprising result was that our targets in the LPF were confirmed as emission-line objects, but none of them is a PN. If we expose long enough, a PN must show not only [O III] λ5007, but also [O III] λ4959, which is three times weaker. In none of our sources could we find the second [O III] line. The spectra show only a strong, isolated and narrow emission line at wavelengths from 5007 to 5042 Å (encompassing the full width of the on-band discovery filter), and nothing else.

Of the 2 QSO or starburst candidates, one was confirmed as a QSO at z = 3.13, showing a typical broad-lined Lyα and several other emissions, including C IV λ1550. The other one appears to be a starburst region (one strong, isolated and narrow emission line, with faint continuum).

In this way we found ourselves unable to work on the expected intracluster PNs, and facing a different problem, namely, we had to identify the isolated emission. Was it [O II] λ3727 at $z = 0.35$, or could it be Lyα at $z = 3.13$? We defined a new MOS configuration, placing the slitlets so as to cover as much wavelength range towards the infrared as possible. We were able to take three exposures with this new MOS configuration. Based on the absence of any other emission line in our spectra, we could rule out all the alternatives, e.g. if the detected emission were [O II] λ3727 redshifted into the on-band filter, then we should see other features, like Hβ, the [O III] lines and Hα, at the corresponding redshift. A similar argument can be used to reject Mg II λ2798 at $z = 0.79$. There is only one possible identification: Lyα at $z = 3.13$. We had unwillingly found a nice collection of high-redshift Lyα emitters, which was an adequate compensation for the loss of the expected intracluster PNs.

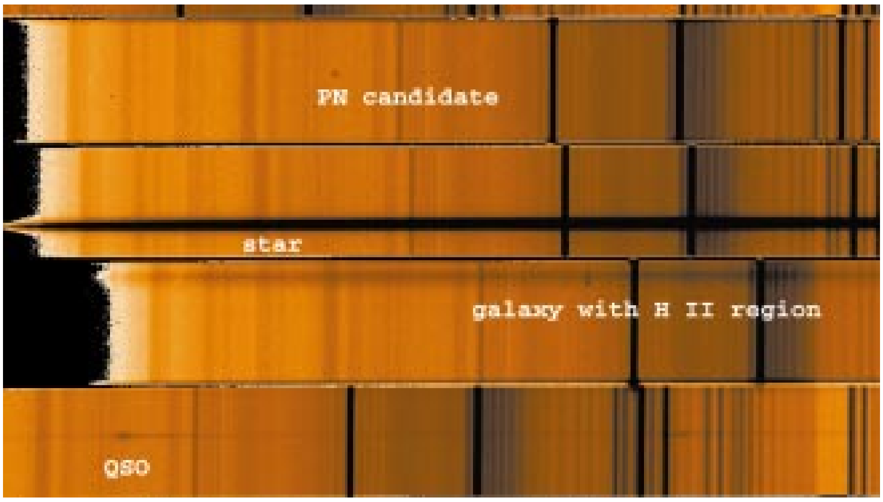

Figure 1. A section of an image produced by coadding 3 MOS exposures of the La Palma Field (LPF), taken with FORS. Here 4 of the 19 FORS slitlets are shown. These spectra, taken during new moon, are dominated by strong sky emissions. From top to bottom: (1) one of our intracluster PN candidates, now re-identified as a high-redshift Lyα emitter; (2) a foreground star; (3) a low-redshift galaxy showing a bright H II region at the edge, where Hβ and the [OIII] emissions λλ4959, 5007 are visible; (4) one of the QSO or starburst candidates, confirmed as a QSO. The strong and broad emission line is Lyα at z = 3.13. A weak continuum is visible. C IV λ1550 is visible to the right, flanked by strong sky emissions.

4. How Could This Happen?

Not just a few, but all the sources we tested with FORS are high-redshift galaxies. However it would be wrong to conclude that intracluster PNs do not exist. In fact, multi-object spectroscopy with the AAT and the 2-degree-field (2df) fibre spectrograph has confirmed the PN nature of many Virgo intracluster candidates, by detecting both [O III] emissions at 4959 and 5007 Å (Freeman et al. 1999). What happened to us is that the surface density of intracluster PNs in the LPF appears to be much lower than in other places across the Virgo cluster, probably indicating some degree of clumpiness in the distribution of the diffuse intracluster population. This will be verified by wide field surveys currently in progress.

There is another aspect to consider: the rather small area of the LPF (50 arcmin^2). Given a small area and a low surface density, the total number of intracluster PNs is small, and it becomes very improbable to find bright PNs. It seems that the fraction of high-redshift Lyα sources in the on-band/off-band samples is higher at faint magnitudes, thus explaining the detections in the LPF. We conclude that it is more efficient to search for intracluster PNs using wide-field survey cameras, like the WFI at the ESO 2.2-m telescope. With a larger area the total number of PNs increases and it is more probable to find bright ones; at brighter magnitudes the fraction of high-redshift Lyα emitters is smaller.

5. Properties of the Lyα Emitters

The weak (in most cases undetected) continuum implies a large Lyα equivalent width, between 20 and 200 Å in the rest frame. For these typical equivalent widths the most probable explanation is H II regions ionised by recently formed massive stars (e.g. Chariot and Fall 1993). The observed Lyα fluxes are between 2×10^{-17} and 2×10^{-16} erg cm^{-2} s^{-1}. Adopting $z = 3.13$, $H_0 = 70$ km s^{-1} Mpc^{-1} and $q_0 = 0.5$ we get a luminosity distance of 1.8×10^4 Mpc, which implies Lyα luminosities for our sources between 2×10^8 and 2×10^9 $L_\odot$. These numbers depend on our assumptions about the cosmological parameters: for a flat universe with $\Omega_0 = 0.2$, $\Omega_\Lambda = 0.8$, and the same z and H_0 as above, the luminosity distance becomes 3×10^4 Mpc, and the Lyα luminosities become larger by a factor 2.8. Our Lyα emitters are quite similar to those recently found by Hu (1998), Cowie & Hu (1998) and Hu et al. (1998) at redshifts from 3 to 5.

Using simple population synthesis models, on the assumption that these sources are produced by star formation with a Salpeter initial mass function and a lower mass cut-off of 0.5 $M_\odot$, we have concluded (Kudritzki et al. 1999 *ApJ* submitted) that the nebulae are nearly optically thick and must have a very low dust content, in order to explain the high observed Lyα equivalent widths. These galaxies must differ substantially from the typical Lyman break galaxies detected through their U-dropout; those are characterised by a strong continuum (needed for their very detection) and weak or absent Lyα emission. We attribute this difference to a lower dust content of our objects.

For the cosmological and star formation parameters we adopted, the total stellar mass produced would seem to correspond to the formation of rather small galaxies, some of which are perhaps destined to merge. However, one of our sources might become a serious candidate for a proto-giant spheroidal galaxy if we assumed continuous star formation, a low mass cut-off of 0.1 $M_\odot$ in the IMF, and a flat accelerating universe with $\Omega_0 = 0.2$ and $\Omega_\Lambda = 0.8$.

The implied star formation density in our sampled comoving volume is probably somewhat smaller than, but of the same order of magnitude as, the star formation density at $z \sim 3$ derived by other authors from Lyman-break galaxy surveys (see e.g. Steidel et al. 1999). This result agrees with the expectation that the Lyα emitters are a low-metallicity (or low-dust) tail in a distribution of star-forming regions at high redshifts. Finally, the Lyα emitters may contribute as many H-ionising photons as QSOs and Ly-break galaxies at $z \sim 3$ (see e.g. Madau et al. 1998). They are therefore potentially significant for the ionisation budget of the early universe.

6. Future Work

Now we would like to do some additional work on these Lyα emitters. In particular we would like to use ISAAC; we expect the strongest [O II] and [O III] forbidden lines as well as Hβ to be detectable with the Short Wavelength arm of ISAAC in Medium Resolution spectroscopic mode. This would allow us to either determine or (in the case of non-detection) put an upper limit to the metallicity. It might also be possible to clarify to what extent the production of Lyα photons can be attributed to AGN activity instead of recent massive star formation. The firm detection of an infrared continuum would help to constrain the characteristics and total mass of the stellar populations through comparison with population synthesis models.

References

[1] Arnaboldi M., Freeman K.C., Méndez R.H. et al. 1996, *ApJ* **472**, 145.
[2] Charlot S., Fall S.M. 1993, *ApJ* **415**, 580.
[3] Cowie L.L., Hu E.M. 1998, *AJ* **115**,1319.
[4] Feldmeier J.J., Ciardullo R., Jacoby G.H. 1998, *ApJ* **503**, 109.
[5] Ferguson H.C., Tanvir N.R., von Hippel T. 1998, *Nature* **391**, 461.
[6] Freeman K.C. et al., 1999, in Galaxy Dynamics: from the Early Universe to the Present, ASP Conf. Ser., eds. F. Combes, G.A. Mamon, V. Charmandaris, in press, astro-ph/9910057.
[7] Hu E.M. 1998, ASP Conf Ser. 146, p. 148.
[8] Hu E.M., Cowie L.L., McMahon R.G. 1998, *ApJ* **502**, L99.
[9] Hui X., Ford H.C., Freeman K.C., Dopita M.A. 1995, *ApJ* **449**, 592.
[10] Jacoby G.H., Ciardullo R., Ford H.C. 1990, *ApJ* **356**, 332.
[11] Madau P., Haardt F., Rees M.J. 1998, preprint astro-ph/9809058 (4 Sep 1998).
[12] Méndez R.H., Guerrero M.A., Freeman K.C. et al. 1997, *ApJ* **491**, L23.
[13] Steidel C.C., Adelberger K.L., Giavalisco M. et al. 1999, preprint astroph/ 9811399v2 (23 Jan 1999).
[14] Thompson D., Djorgovski S., Trauger J. 1995, *AJ* **110**, 96.

E-mail: kudritzki@usm.uni-muenchen.de

VLT Spectroscopy of the *z* = 4.11 Radio Galaxy TN J1338–1942

C. DE BREUCK[1,2], W. VAN BREUGEL[2], D. MINNITI[2,3], G. MILEY[1], H. RÖTTGERING[1], S.A. STANFORD[2] and C. CARILLI[4]

[1]Sterrewacht Leiden, The Netherlands (debreuck,miley,rottgeri@strw.leidenuniv.nl)
[2]Institute of Geophysics and Planetary Physics, Lawrence Livermore National Laboratory, Livermore, U.S.A. (wil,adam@igpp.llnl.gov)
[3]P. Universidad Católica, Santiago, Chile (dante@astro.puc.cl)
[4]National Radio Astronomy Observatory, Socorro, USA (ccarilli@nrao.edu)

High-redshift radio galaxies (HzRGs) play an important role in cosmology. They are likely to be some of the oldest and most massive galaxies at high redshifts, and can therefore constrain the epoch at which the first generation of stars were formed. The near-IR Hubble $K-z$ diagram of powerful radio galaxies shows a remarkably tight correlation from the present time out to $z = 5.19$, despite significant *K*-corrections (van Breugel et al. 1998, 1999). This indicates that we can follow the evolution of the hosts of HzRGs from near their formation epoch out to low redshift ($z \lesssim 1$), where powerful radio sources inhabit massive elliptical galaxies (e.g. Lilly & Longair 1984; Best, Longair & Röttgering 1998). For example, at $z \sim 3$, we observe a change in the observed K-band morphologies of HzRGs from large-scale low-surface brightness emission with bright radio-aligned clumps at $z \lesssim 3$ to smooth, compact structures, sometimes showing elliptical shapes, like their ocal Universe counterparts (van Breugel et al. 1998). These surrounding clumps have properties similar to the UV dropout galaxies at similar redshifts (Pentericci et al. 1999), and indicate that HzRGs often reside in (proto-)cluster environments. This evolution picture seems consistent with the hierarchical clustering formation models (e.g. Kauffmann et al. 1999), where massive objects form by accretion of smaller systems located in over-dense regions.

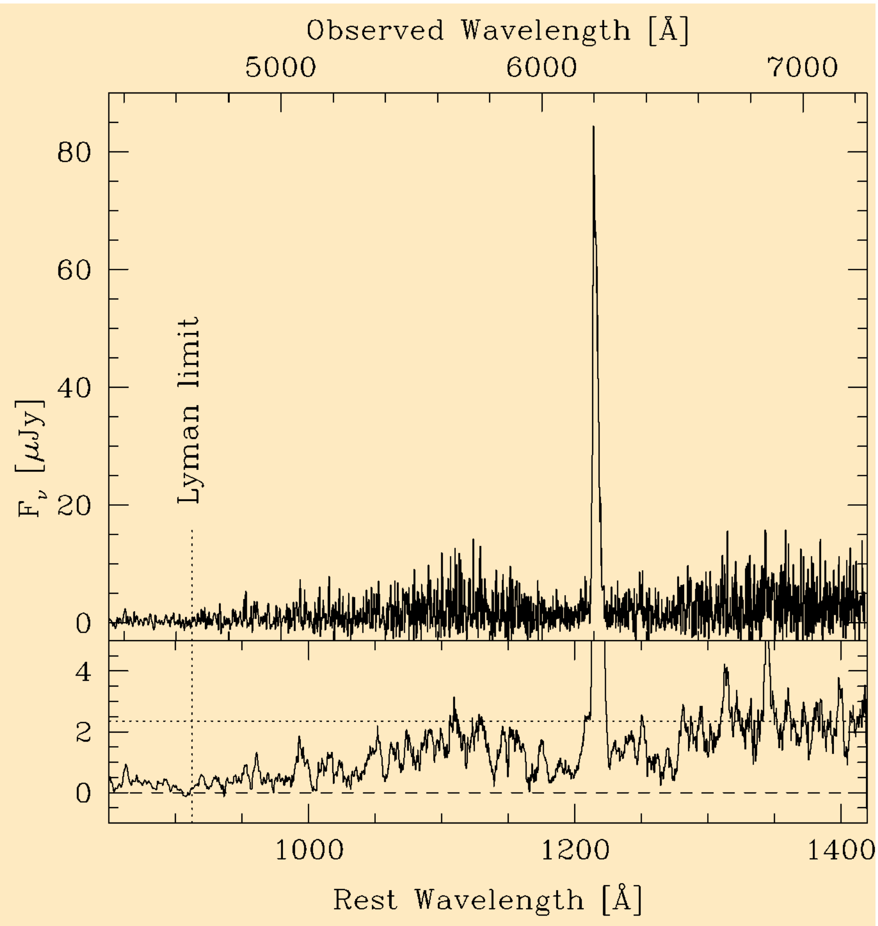

Figure 1: VLT spectrum of TN J1338–1942. The lower panel has been boxcar smoothed by a factor of 9 to better show the shape of the Lyα forest and the Lyman limit.